Development of a Photogrammetric 3D Measurement System for Small Objects Using Raspberry Pi Cameras as Low-Cost Sensors

Thomas P. Kersten[1], Florian Timm[1] & Kay Zobel[1]

[1] HafenCity University Hamburg, Photogrammetry & Laser Scanning Lab
Henning-Voscherau-Platz 1, D-20457 Hamburg, Germany
[Thomas.Kersten, Florian.Timm, Kay.Zobel]@hcu-hamburg.de

Keywords: 3D, comparison, coded targets, multi-camera, synchronisation, system calibration, structure-from-motion.

Abstract

The digitisation of cultural objects in museums presents two distinct opportunities. Firstly, it allows for the preservation of the objects and collections themselves. Secondly, it enables their accessibility to the general public as 3D models in virtual exhibitions on the Internet. Cultural artefacts of significance can be recorded using laser scanners, 3D handheld scanners or photogrammetry employing the structure-from-motion method. In order to efficiently record and model the considerable number of culturally significant objects, automated recording systems and automated evaluation processes are required.
This article presents a low-cost photogrammetric measurement system developed at HafenCity University Hamburg. The system comprises 24 Raspberry Pi cameras mounted on an aluminium frame, which enables the automatic and time-synchronous digitisation of small objects. To ascertain the veracity of the point clouds generated for the test objects, a comparison was conducted with the reference data obtained from the high-precision ATOS 5 structure light projection system. It was established that comprehensive coverage and a high degree of precision could only be achieved through the incorporation of a turntable and supplementary images of the objects, necessitated by minor rotations. The configuration of the photogrammetric low-cost measurement system and the requisite camera calibrations are delineated in the article.

1. Introduction

Today, there is a clear and pressing need to capture three-dimensional models easily and cost-effectively in many fields, such as 3D modelling in archaeology, the games and film industries, or in industry for development and quality control. In the context of museums, there is a clear need to digitise exhibits with the objective of presenting them online in virtual exhibitions. It is also important to document and research the exhibits. It is crucial to recognise that cultural artefacts are vulnerable to loss or damage from a range of causes, including natural disasters, vandalism, fires and armed conflicts. The digitisation of these objects is an effective method of preserving them and making them accessible to the public. However, in addition to precautionary digitisation, it is also essential to record objects promptly after damage has occurred.

Optical measurement methods such as photogrammetry and laser scanning are the most efficient and contactless way of recording these objects. HafenCity University Hamburg has developed a photogrammetric measurement system for small objects (up to 40 cm in diameter). The system comprises 24 low-cost Raspberry Pi cameras (Figure 1). This involved investigating the number of cameras required, the arrangement of the cameras, the technical recording parameters (e.g. camera constant, distortion, etc.) and the synchronisation of the cameras. Furthermore, a procedure for calibrating the cameras was developed. The images are automatically transferred to the analysis software, where 3D point clouds and textured 3D models are generated using the commercial software package Agisoft Metashape. The image data can also be processed with the open source software OpenDroneMap (https://www.opendronemap.org/). The photogrammetric images are scaled using calibrated control points (ring coded targets and ArUco marker) and various scales in object space, which can be automatically and clearly measured in the image data.

A series of general requirements have been defined to facilitate the development of a low-cost photogrammetric system. The system must be able to record small objects with a diameter of up to approximately 40 cm through automatic image capture. It must also be straightforward to use and cost-effective. The prototype should be easily replicated, and open-source software should be a viable option. Beyond that, the system should be portable and functional in other countries, and its capabilities should be expandable.

Furthermore, the following functional options were required. (1) The cameras must be triggered simultaneously or with minimal delay. (2) The system must be controllable independently of other devices, for example via button control. (3) The system status must be easily recognisable even without connecting a computer. (4) Control points must be automatically identified and used to determine the exterior orientations of the images. (5) The images must be sharp and focused, and (6) the exposure must be automatic, but the brightness of the images must be identical. Furthermore, the recorded data must be stored internally, while the storage on portable storage media such as USB sticks must be possible. However, a direct data transfer to Structure-from-Motion (SfM) software including automated processing of images into a 3D model must be implemented.

The system must be designed to operate independently of network connections. Only a system-owned WiFi router is required for internal communication.

2. Related Work

The current market offers an extensive range of software packages for 3D reconstruction of objects of varying dimensions. It is important to note that a subset of these software packages is open source. In a comparative study presented by Kersten and Lindstaedt (2012), the authors definitively demonstrated the use of open-source software and web services for the automatic reconstruction of 3D objects from multiple images. The study focused on three distinct domains: architectural, cultural heritage, and archaeological applications. Schöning and Heidemann (2015) evaluated multi-view 3D reconstruction software, while Olagoke et al. (2020) presented a comprehensive literature survey on multi-camera systems and their applications. Nikolov and Madsen (2016) conducted a definitive benchmarking study of close-range SfM 3D reconstruction software under varying capturing conditions. The same research group quantified the influence of surface texture and shape on SfM 3D reconstructions (Nielsen et al., 2022). Kersten et al. (2016a) initiated investigations into the potential of low-cost systems (DAVID SLS-1 and Microsoft® Kinect) for 3D reconstruction of small objects.

3. Reference Bodies

The following reference objects were used for the benchmarking test (Figure 1): a plaster bust of Einstein (height 160 mm), a Moai figure from Easter Island (height 140 mm) and a so-called "Testy" (height 380 mm) from the Institute of Computer Science at the Humboldt University in Berlin (Reulke & Misgaiski, 2012). All three test objects were scanned using a high-precision structured light system, ATOS 5, developed by Carl Zeiss GOM Metrology, for comparison. This system is designed for high-speed 3D scanning, fast data processing and higher resolution (Carl Zeiss GOM Metrology, 2024). The ATOS 5 has a system precision of 10-30 microns, uses a LED as a light source, and has a measuring area of 170×140 - 1000×800 mm, a working distance of 880 mm and is capable of measuring up to 12 million points per scan. The two reference bodies, Testy and Einstein's bust, have already been used to analyse the geometric accuracy of handheld 3D scanners (Kersten et al., 2016a & 2016b; Kersten et al., 2018), while Testy and Einstein's bust have also been used to analyse the geometric accuracy of low-cost systems (Kersten et al., 2016a; Kersten et al., 2024).

Figure 1. Reference objects (Moai figure, Einstein bust, and Testy) for testing the multiple Raspberry Pi cameras setup.

4. Multi Camera System Setup

The Raspberry Pi Camera Module 3 was utilized as the camera (c = 4.74 mm), which is operated by a Raspberry Pi Zero W. In comparison to other low-cost cameras, such as webcams or the ESP32 CAM, the cameras have a high geometric resolution of 12 megapixels (4608×2592 pixels) and relatively large pixels of 1.4 µm (Raspberry Pi Foundation, 2023), which, subjectively, results in excellent image quality. The camera has motorised focus from 10 cm to infinity, a field of view of 66°×41° and a f-stop of F1.8. The number of cameras for the prototype was defined in conjunction with the type of frame. This was achieved by modelling the frame setup and its cameras in 3D visualisation software Blender (Figure 2, top left), and rendering the individual images of the potential camera positions. The cameras were mounted on the frame at an angle of 90° so that they could still be shifted and rotated in a vertical direction. Figure 2 (top right) shows the stable aluminium frame for mounting the cameras, while Figure 2 (bottom) illustrates the complete structure of the system. Figure 3 (left) depicts a Raspberry Pi camera with the mounting bracket.

Figure 2. Design of the photogrammetric low-cost 3D measurement system (top left) and realised aluminium frame (top right). Setup of the photogrammetric low-cost 3D measurement system using 24 Raspberry Pi cameras (bottom).

In order to produce the best possible images, it is essential that the object is sufficiently and evenly illuminated. Individually controllable LED light strips were attached to the aluminium rods as a light source (Figure 3, centre), allowing individual areas to be switched off, for example, in order to reduce glare. Furthermore, different light colours can be set in order to enable status messages or to influence the lighting of the object (Figure 3, right). The system is controlled by Raspberry Pi 4, which also controls the cameras. To mitigate the impact of external light sources, a fabric cover was positioned over the aluminium frame (Figure 5, left). The total cost of the materials for the system setup, including the power supply, was 2000 EUR, which can be considered a cost-effective low-cost photogrammetric system.

Figure 3. Raspberry Pi camera with the mounting bracket (left), low-shadow lighting due to LED strips (centre), coloured lighting to indicate system status (right).

To automate the measurement of image points and orientate the images, as well as to calibrate the cameras, ArUco targets (Figure 4, left) were placed in object space as control points. These were generated by OpenCV (Hu et al., 2019), while on the other hand approximately concentric circular coded targets (CCCT) (Figure 4 right) were distributed in object space (Figure 8, left). These ring codes (Schneider and Sinnreich, 1992; Liu et al., 2021) were employed as tie points in the bundle adjustment.

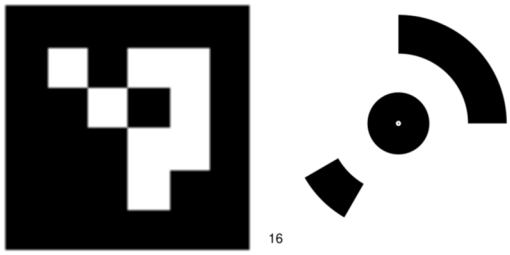

Figure 4. ArUco target (left) and concentric circular coded targets (right).

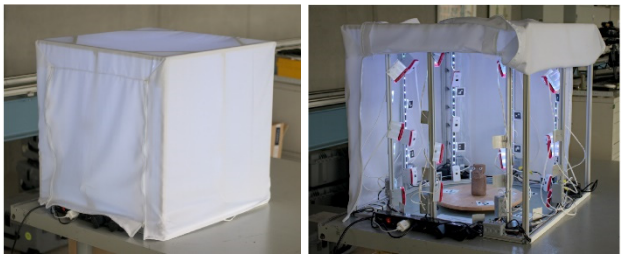

Figure 5. Setup of the photogrammetric low-cost 3D measurement system with fabric cover (left) and details of the illumination and camera mount without fabric cover (right).

5. System Calibration

In order to calculate 3D models with accurate scaling, it is necessary to determine a number of parameters. In addition to establishing the interior orientation of the cameras, it is also essential to ascertain the scale of the image data sets. A combination of calibrated scale bars and control point coordinates in object space was selected as the most appropriate method for determining the scaling (Figure 8, left).

Preliminary investigations have revealed that the camera calibration of the Raspberry Pi cameras is not stable. In investigations conducted with older Raspberry Pi cameras (normal angle lens with camera constant c = 3.6 mm, 5 MP, 4 µm pixel size of the OmniVision OV5647 type), the following results were obtained through repeat measurements (Kersten et al., 2016c): (1) The camera constant c is observed to vary only slightly and is thus assumed to be relatively stable. (2) Conversely, the position of the image centre point is found to exhibit significant differences of up to 50 µm. (3) The radial-symmetric distortion (k_1, k_2) is observed to vary only slightly and appears to be relatively stable. (4) No clear trend is identified for the other parameters (scale and shearing as well as radial-asymmetric and tangential distortion).

Given the shallow depth of field of the cameras used, investigations were previously conducted using various commercial software to ascertain whether a superior 3D model could be created using focus stacking. The tests were unsuccessful, but the technique had been demonstrated to be effective by other authors (Clini et al., 2016) for the survey of small objects using a Nikon D810 SLR camera, offering excellent results and high-definition 3D models. Further investigation is therefore warranted.

The simultaneous triggering of all cameras was also analysed using a stopwatch with a display of hundredths of a second. The synchronised images from three test series each exhibited a maximum deviation of 0.2 seconds between the first and last image, indicating that the cameras are synchronised for the intended application. However, this can be neglected for static objects.

The cameras in question lack stable interior orientation parameters, which precludes calibration to determine fixed parameters. As the interior orientation, particularly the camera constant, is linearly dependent on focusing, a formula for approximating interior orientation values as a function of focusing was developed. The actual determination of the internal orientation parameters is conducted during operation in the form of a simultaneous calibration, with the initial values serving as starting values for the bundle block adjustment. Consequently, the images were captured using five distinct image-focusing techniques, each employing 24 Raspberry Pi cameras. Subsequently, the images were automatically orientated in Agisoft Metashape using ArUco targets (Hu et al., 2019), the position of which was determined in advance through bundle adjustment using the scale bars. Furthermore, approximately 100 targets bearing ring codes (Schneider and Sinnreich, 1992; Liu et al., 2021) were distributed in object space and employed as tie points (Figure 8, left). In Metashape, all images with the same focusing (in total five groups) were assumed to have been captured by a single camera, and the interior orientation parameters were determined. Subsequently, each camera parameter was adjusted individually. This two-stage procedure has the effect of gradually improving the initial values. In contrast, a single-step procedure without initial values resulted in the generation of erroneous values. The interior orientation parameters were determined through the calculation of the camera constant, principal point shift and distortion. The results of the adjustments demonstrate that the camera constant c is linearly dependent on the focusing, exhibiting a strong correlation between the two variables. However, the dependence is not statistically significant for the principal point x_0', y_0' and the radial-symmetric distortion k_1, k_2, k_3.

6. Image Data Acquisition and Results

Once the design and construction of the prototype were complete, a series of tests were conducted to ascertain the accuracy of the system and to determine the optimal number of cameras to be included in the system. The recordings are initiated by means of a software button on the desktop software, the web interface, or a button. The camera exposures are synchronised, thereby generating images. The Raspberry Pi Zero W sends the images and the detected and measured ArUco markers to the Raspberry Pi 4, which calculates the camera positions and stores the data. The desktop software then downloads the data and transfers it to the SfM software Agisoft Metashape (version 1.8.5) or OpenDroneMap, which generates a point cloud and the 3D model of the captured object. The complete workflow, from the acquisition of the data to its processing, is shown in a diagram in Figure 6.

The test objects employed for the acquisition of image data were a small Moai figure, an Einstein bust, and the test body Testy (Figure 1). As previously stated, these three test bodies were scanned using the high-precision structure light system Zeiss GOM ATOS 5 (system precision 10-30 microns) as a reference.

It can be posited that the measurements obtained from the structure light projection system are of a markedly higher precision than those obtained from the prototype system. It can thus be assumed that the measurements obtained from the structure light projection system represent quasi-true values. It should be noted that the aforementioned assumption does not apply to the positions of the tie points, which were marked with circular markers on each test object (see Figure 7). These were attached for measurement with the ATOS 5 in order to connect the various scans. The structured light system automatically recognises these targets, and these areas in the generated 3D model are interpolated. However, this can result in significant deviations if the surface is not flat or the thickness of the tie point markers is not correctly specified in the software of the structured light system.

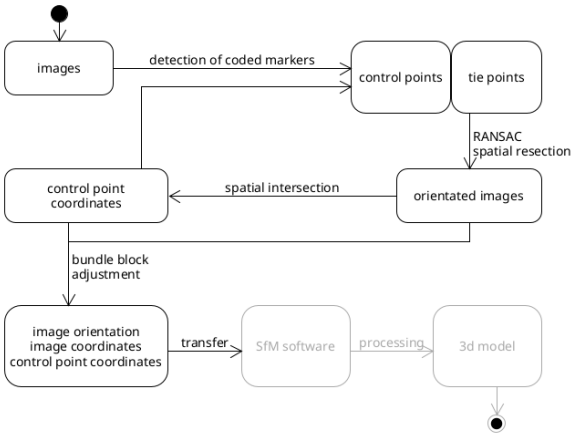

Figure 6. Workflow for the data acquisition and processing.

The a priori estimated precision for the discrepancies from the reference data was projected to be within a range of 0.03 mm to 0.15 mm in the position X, Y and 0.02 mm to 0.25 mm in the depth coordinate Z. The depth coordinate Z is based on the distance of 10-50 cm, the camera constant, the resulting photo scale, a basis of 30 cm between two cameras and the image measurement precision of approximately 1 pixel (Timm, 2024).

The three test objects were recorded with the prototype and the data subsequently processed in Agisoft Metashape. Subsequently, the modelled surface from the structured light projection system and the point cloud from the prototype were superimposed in CloudCompare (Girardeau-Montaut, 2024), thereby enabling the calculation of the differences (M2C - Mesh to Cloud). In the visualisation of the differences, some systematic deviations can be seen in Figure 7 due to the narrow range from -0.6 mm to 0.6 mm, i.e. depending on the model, some areas were not recorded at all due to a lack of nadir-looking cameras and others deviate significantly from the expected accuracy.

The results of the 3D comparison between the reference meshes and point clouds of the test objects including the average deviation, Root Mean Square Error (RMSE) and maximum deviation are summarised in Table 1. Additionally, the Moai figure was recorded manually by a Nikon D90 with a 50 mm lens in 144 images for comparison with a DSLR camera. The Nikon D90 results show higher average deviation, similar RMSE, but significantly better maximum deviation. However, the results for the other two test objects (RMSE and max. deviation) are less favourable than those for the Moai.

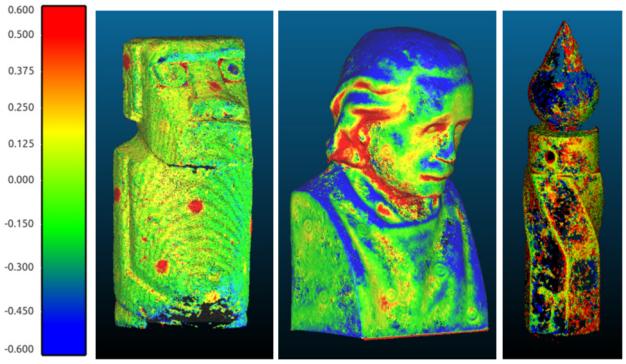

Figure 7. Visualisation of the deviations between reference data (mesh) and point clouds of the three test objects.

Object	Ø deviation	RMSE	max. dev.
Moai	-0.024 mm	0.16 mm	2.6 mm
Moai (no marker)	-0.038 mm	0.14 mm	2.6 mm
Moai (Nikon D90)	0.255 mm	0.15 mm	1.3 mm
Einstein bust	0.001 mm	0.36 mm	-3.6 mm
Testy	-0.047 mm	0.64 mm	11.6 mm

Table 1. First results of the 3D comparison between reference meshes and point clouds of the test objects.

In order to improve the quality of the digitisation of the test objects, an alternative approach was adopted whereby a turntable was utilised for the images, thus enabling each camera to capture more than one image of the object. This method was employed in lieu of increasing the actual number of cameras, which would have been a more expensive and complicated solution.

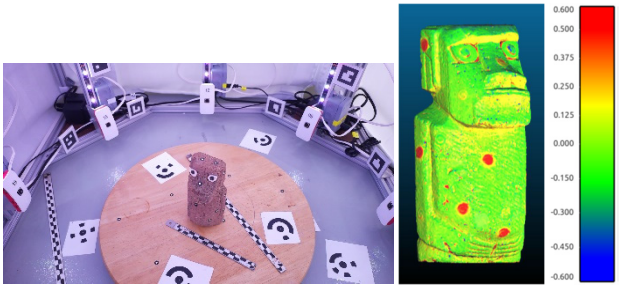

Figure 8. Moai figure on the turntable in the low-cost photogrammetric 3D measurement system (left) and sketch of the camera setup indication the rotation steps (right)

Object Moai	Ø dev. [mm]	RMSE [mm]	Max. dev. [mm]	# points [Mill.]
no turntable	-0.03	0.22	2.0	3.3
with turntable	-0.03	0.15	1.6	3.4
Nikon D90	0.03	0.17	1.2	0.05

Table 2. Results of the 3D comparison between reference meshes and point clouds of the Moai figure using the turntable.

The utilisation of the turntable resulted in a notable enhancement of the 3D point cloud of the Moai in comparison to Figure 7. This was characterised by a reduction in deviations and an increase in completeness (Figure 8 centre). The reduction in average deviations can be attributed to the automated adjustment of the scale (Table 2). is highly comparable to the Nikon D90 data set, with minimal alteration in the number of points. In comparison to the comprehensive model of the DSLR camera, it is evident that no substantial assertions can be made regarding the extent of the object's coverage.

Object Moai	No.	# cameras	rotation	# photos	RMSE	max dev	# points	coverage	correct
ATOS 5							346 830	100%	100%
Standard	a	24	1	24	0.18 mm	2.52 mm	628 727	93.1%	99.9%
Fine rotation	b	24	4×1/32	96	0.14 mm	1.42 mm	758 364	100.2%	100.0%
Rough rotation	c	24	5×1/8	120	0.16 mm	1.42 mm	777 533	98.8%	100.0%
2 of 3 cameras	d	16	1	16	1.20 mm	7.74 mm	596 979	68.4%	70.4%
Each 2nd camera	e	12	1	12	0.49 mm	4.01 mm	346 830	54.9%	94.1%
… with rotation	f	12	2×1/8	24	0.25 mm	1.44 mm	760 538	95.7%	99.8%
One plane	g	6	4×1/8	24	1.57 mm	1.44 mm	753 062	77.8%	68.6%
… with markers	h	6	5×1/8	30	0.29 mm	2.50 mm	640 810	94.2%	98.9%

Table 3. Results of the 3D comparison between reference meshes and point clouds of the Moai figure using the turntable in various rotation configurations.

A series of camera configurations were tested in order to ascertain the number of cameras required for optimal accuracy. In order to achieve this, the Moai was employed, with a number of cameras deactivated in Agisoft Metashape, resulting in a recalculation of the dense 3D point cloud. Subsequently, the results were compared with those obtained using the ATOS 5 system in the CloudCompare software. Furthermore, the coverage and accuracy of the point cloud were evaluated as additional parameters (Table 3). The distribution of cameras employed in each instance is illustrated in Figure 9. The points displayed in pink represent the active cameras. The tests demonstrated that the utilisation of the turntable led to a notable enhancement in object coverage and elevated accuracy, attributable to the augmented number of images. The most favourable outcome of the comparison between the point cloud and the reference data was an average deviation of 0.14 mm and a maximum deviation of 1.4 mm. This was achieved through the utilisation of a turntable with four image acquisitions in 1/32 rotation steps, which corresponds to 96 photos in total (Figure 9 and Figure 10).

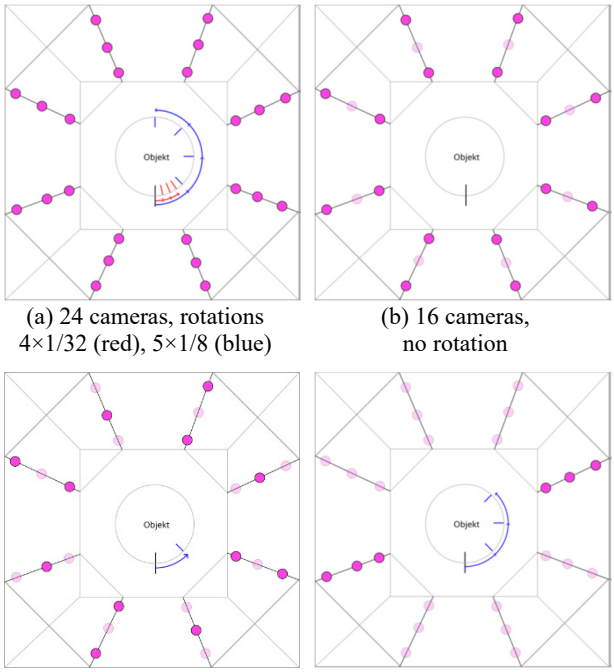

(a) 24 cameras, rotations 4×1/32 (red), 5×1/8 (blue)

(b) 16 cameras, no rotation

(c) 12 cameras, rotations 2×1/8 (blue)

(d) 6 cameras, rotations 4×1/8 (blue)

Figure 9. Positioning of the cameras (active in pink) and the utilised positions of the turntable (in blue and red), as observed from an overhead perspective.

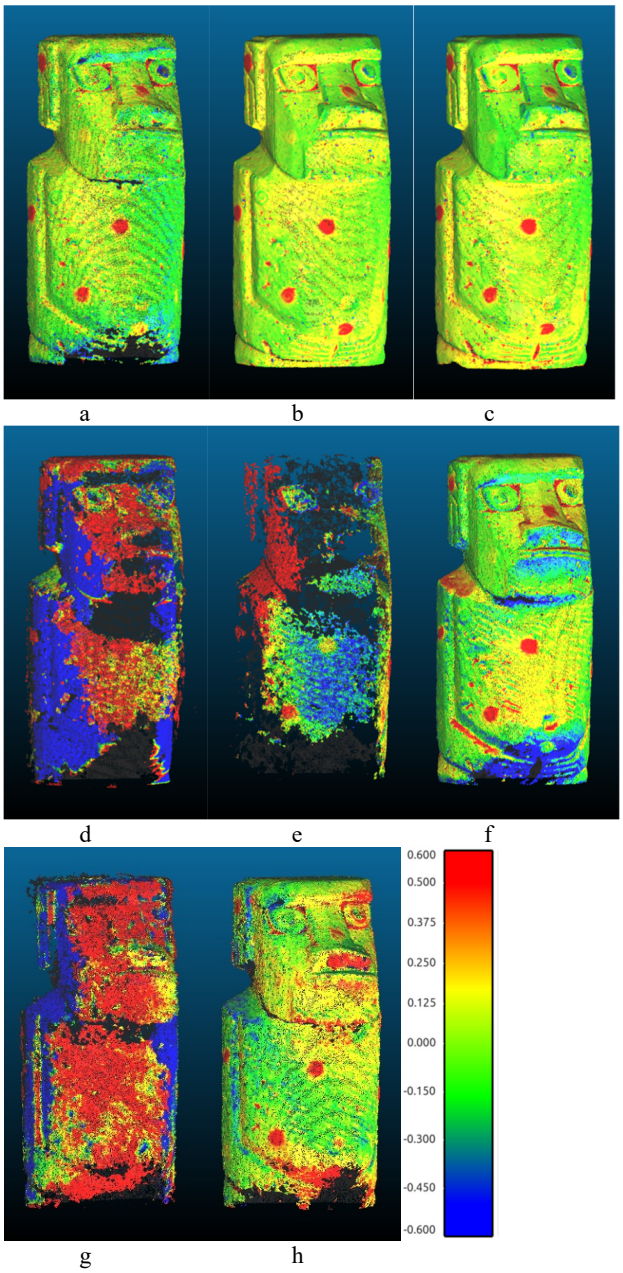

Figure 10. Coloured visualisation of the deviations of the point clouds of the Moai figure from the reference data (red: +0.6 mm, blue: -0.6 mm) using different camera configurations as specified in Table 3.

Furthermore, the extent to which the object surface was covered by points was evaluated as a supplementary criterion. To this end, the point clouds were filtered to include only those that were less than one millimetre away from the meshed model of the structured light projection system. Subsequently, the point density was reduced to 1 mm, and the number of points was counted. The number of these points was then related to the number of the reference data set, which was determined in the same manner. This enabled an evaluation of the extent to which the surface was covered. A coverage of 100% indicates that both thinned point clouds have the same number of points and that the data set covers the surface of the reference data set in a similar manner. Furthermore, the proportion of accurately positioned points was evaluated independently of the total number of points. In this case, a value of 100% indicates that all points are correctly aligned or within a maximum of 1 mm of the surface of the reference data.

As expected, the quality and coverage of the point cloud decreased in direct proportion to the reduction in the number of cameras used. In one recording with all 24 cameras, 93% of the surface area (without ground) was covered (Figure 10a). With 18 cameras (Figure 10d), the coverage was 68%, and with 12 cameras (Figure 10e), it was 54%. Even with 18 cameras, the Moai was barely recognisable, and with 12 cameras, it was no longer recognisable. These results suggest that a high number of cameras is appropriate for this object, provided no turntable is used.

7. Conclusion and Outlook

The project demonstrated that a photogrammetric measurement system based on Raspberry Pi cameras can be developed as a low-cost system. Furthermore, it was shown that the additional use of a turntable to capture the test object from different perspective views can increase the coverage of the object and the accuracy of the 3D point cloud.

The system was found to achieve the intended accuracy, with a range of 0.1 mm to 0.5 mm depending on the test object. The number of 24 cameras was sufficient for the majority of objects tested. However, experiments with fewer cameras resulted in poor coverage of the object, leading to the omission of areas in the point cloud. It is therefore recommended that the use of the turntable be employed to further increase accuracy and improve object coverage in instances where the number of cameras cannot or should not be increased.

The requirements formulated and defined for the photogrammetric low-cost measurement system in Chapter 1 were largely fulfilled. Nevertheless, further examination of the prototype on a diverse array of additional objects is essential to substantiate its practical viability. In the future, the coverage of the object surface and thus the result can be improved by two additional nadir-viewing cameras on top of the box.

Acknowledgements

The authors would like to express their gratitude to Ingo Jahn and Claudia Rajczak of GDV Systems + Solutions GmbH in Bad Schwartau, Germany, for undertaking the scanning of the reference bodies using the ATOS 5 structured light system.

References

Clini, P., Frapiccini, N., Mengoni, M., Nespeca, R., Ruggeri, L., 2016. SfM technique and focus stacking for digital documentation of archaeological artifacts. *Int. Arch. Photogramm. Remote Sens. Spatial Inf. Sci.,* XLI-B5, 229-236, doi.org/10.5194/isprsarchives-XLI-B5-229-2016.

Girardeau-Montaut, D., 2024. CloudCompare - 3D point cloud and mesh processing software. Open Source Project. http://www.cloudcompare.org/, last access November 03, 2024.

Hu, D., DeTone, D., Malisiewicz, T., 2019. Deep ChArUco: Dark ChArUco Marker Pose Estimation. *Proceedings of the IEEE/CVF Conference on Computer Vision and Pattern Recognition*, 8436-8444.

Kersten, T., Lindstaedt, M., 2012. Automatic 3D Object Reconstruction from Multiple Images for Architectural, Cultural Heritage and Archaeological Applications Using Open-Source Software and Web Services. *PFG - Journal of Photogrammetry, Remote Sensing and Geoinformation Science*, 2012(6), 727-740.

Kersten, T., Omelanowsky, D., Lindstaedt, M., 2016a. Investigations of low-cost systems for 3D reconstruction of small objects. Digital Heritage - Progress in Cultural Heritage: Documentation, Preservation, and Protection: 6th International Conference, EuroMed 2016, *Lecture Notes in Computer Science*, 10058, 521-532, Springer International Publishing, Cham. doi.org/10.1007/978-3-319-48496-9_41.

Kersten, T., Przybilla, H.-J., Lindstaedt, M., Tschirschwitz, F., Misgaiski-Hass, M., 2016b. Comparative Geometrical Investigations of Hand-Held Scanning Systems. *Int. Arch. Photogramm. Remote Sens. Spatial Inf. Sci.,* XLI-B5, 507-514. doi.org/10.5194/isprs-archives-XLI-B5-507-2016.

Kersten, T., Sönksen, L., Przybilla, H.-J., 2024. Geometric Accuracy Investigations of Mobile Phone Devices in the Laboratory using High-Precision Reference Bodies. *Int. Arch. Photogramm. Remote Sens. Spatial Inf. Sci.*, XLVIII.

Kersten, T., Stallmann, D., Tschirschwitz, F., 2016c. Development of a new low-cost indoor mapping system – system design, system calibration and first results. *Int. Arch. Photogramm. Remote Sens. Spatial Inf. Sci.,* XLI-B5, 55-62. doi.org/10.5194/isprs-archives-XLI-B5-55-2016.

Kersten, T., Starosta, D., Lindstaedt, M., 2018. Comparative Geometrical Accuracy Investigations of Hand-held 3D Scanning Systems - An Update. *Int. Arch. Photogramm. Remote Sens. Spatial Inf. Sci.,* XLII-2, 487-494. doi.org/10.5194/isprs-archives-XLII-2-487-2018.

Liu, Y., Su, X., Guo, X., Suo, T., Yu, Q., 2021. A Novel Concentric Circular Coded Target, and its Positioning and Identifying Method for Vision Measurement under Challenging Conditions. *Sensors,* 21(3), MDPI, Basel, Schweiz, doi.org/10.3390/s21030855.

Nikolov, I., Madsen, C., 2016. Benchmarking Close-range Structure from Motion 3D Reconstruction Software under Varying Capturing Conditions. *Lecture Notes in Computer Science*, 10058, 15-26, Springer International Publishing, Cham, doi.org/10.1007/978-3-319-48496-9_2.

Nikolov, I., Madsen, C., 2016. Benchmarking Close-range Structure from Motion 3D Reconstruction Software under Varying Capturing Conditions. *Digital Heritage. Progress in Cultural Heritage: Documentation, Preservation, and Protection*, Ioannides et al. (eds.), *Lecture Notes in Computer Science*, 10058, 15-26, Springer International Publishing, Cham, doi.org/10.1007/978-3-319-48496-9_2.

Olagoke, A. S., Ibrahim, H., Teoh, S. S., 2020. Literature Survey on Multi-camera System and its Application. *IEEE Access*, 8, 172892-172922. doi.org/10.1109/ACCESS.2020.3024568.

Raspberry Pi Foundation, 2023. Raspberry Pi Documentation - Camera. Raspberry Pi Foundation, Cambridge, UK, https://www.raspberrypi.com/documentation/accessories/camera.html, last access June 26, 2024.

Reulke, R., Misgaiski, M., 2012. Test body "Testy" for Laser Scanning and Optical Systems. *PFG - Journal of Photogrammetry, Remote Sensing and Geoinformation Science*, 2012(6), zum Titelbild.

Schneider, C.-T., Sinnreich, K., 1992. Optical 3-D Measurement Systems for Quality Control in Industry. *Int. Arch. Photogramm. Remote Sens. Spatial Inf. Sci.,* XXIX, 56-59, https://www.isprs.org/proceedings/xxix/congress/part5/56_xxix-part5.pdf.

Schöning, J., Heidemann, G., 2015. Evaluation of Multi-view 3D Reconstruction Software. *Computer Analysis of Images and Patterns,* CAIP 2015, Azzopardi, G., Petkov, N. (eds), *Lecture Notes in Computer Science*, 9257, 450-461, Springer International Publishing, Cham. doi.org/10.1007/978-3-319-23117-4_39.

Timm, F., 2024. Aufbau eines photogrammetrischen Messsystems mit Raspberry-Pi-Kameras als Low-Cost-Sensoren für die Aufnahme von kleinen Objekten. Master thesis, master study programme Geodesy and Geoinformatics, HafenCity University Hamburg, 95 p.